Discordant Potassium-Argon Model and Isochron "Ages" for Cardenas Basalt (Middle Proterozoic) and Associated Diabase of Eastern Grand Canyon, Arizona

Steven A. Austin, PhD,
Institute for Creation Research, PO Box 2667, El Cajon, California, 92021, USA.

Andrew A. Snelling, PhD,
Answers in Genesis, PO Box 6302, Acacia Ridge DC, Qld. 4110, Australia.*

*current address: Answers in Genesis, PO Box 510, Hebron, Kentucky, 41048, USA.

Abstract

For more than twenty years it has been known that the Rb-Sr and K-Ar systems give discordant "ages" for Cardenas Basalt and associated Proterozoic diabase sills and dikes of Grand Canyon. Thirteen new K-Ar analyses of Proterozoic mafic rocks of Grand Canyon are added to nine published K-Ar analyses. We report a new fourteen-point K-Ar isochron "age" of 516±30 Ma which is strongly discordant with the published Rb-Sr isochron "age" of 1.07±0.07 Ga for Cardenas Basalt. By more than doubling the K-Ar data set we can test explanations for why the discordance exists. Advocates of the Rb-Sr isochron, recognizing the strong geochemical similarity of rubidium and potassium, have not argued for significant potassium addition to these rocks. Addition of potassium during alteration of these rocks would explain the anomously young K-Ar age, but it would also add rubidium and invalidate the Rb-Sr isochron age. Instead, advocates of the Rb-Sr isochron have argued only for significant argon loss. Two argon loss models (episodic loss and continuous loss) are tested in an attempt to explain why these altered rocks have about half the ^{40}Ar required by the conventional Rb-Sr interpretation. Both argon loss models, although attempting to maintain the assumptions of conventional geochronology, fail to explain the data, especially the new data we offer. Three models are proposed as alternatives to argon loss models, but these invalidate using the K-Ar system as conventional geochronology would assume.

Keywords

Basalt, Diabase, Grand Canyon, Potassium-Argon Dating, Model "Ages", Isochron "Ages", Discordance, Argon Leakage Models, Inheritance, Mixing, Change of Decay

Introduction

The Cardenas Basalt (Figure 1) is a succession of lava flows over 300-m-thick occurring deep within a thick succession of strata in the eastern Grand Canyon, Arizona. The 1.1-billion-year Rb-Sr isochron date for the Cardenas Basalt is widely regarded by geologists as the best "age" yet obtained for Grand Canyon strata (Larson, Patterson, & Mutschler, 1994; McKee & Noble, 1974). That "age" agrees with what most geologists have come to believe about other Precambrian strata and the pervasive mafic intrusive and extrusive magmatism of the Middle Proterozoic of the southwestern United States (Hammond & Wooden, 1990; Heaman & Grotzinger, 1992; Howard, 1991). Although we might suppose that radioisotopes could

definitely date Cardenas Basalt, a significant problem has arisen. Published potassium-argon (K-Ar) "ages" for Cardenas Basalt and Precambrian diabase are significantly younger than their associated rubidium-strontium (Rb-Sr) "ages" (Austin, 1994). Why are K-Ar dates significantly younger than the "accepted" Rb-Sr age? We seek to examine the potassium and argon systematics of Cardenas Basalt along with associated Precambrian diabase dikes and sills. We seek to test theories which explain why K-Ar "ages" are significantly younger than the widely accepted Rb-Sr isochron "age."

Geology of Sills, Dikes, and Flows

Mafic igneous rocks occur as sills, dikes, and flows

in the Upper Precambrian (Proterozoic) Unkar Group of the Grand Canyon, Arizona (Figures 1 and 2). The extrusive rocks form a 300-m-thick flow sequence called the Cardenas Basalt which rests conformably on the Dox Formation in the middle of the 4000-m-thick Proterozoic Grand Canyon Supergroup sedimentary sequence (Hendricks & Stevenson, 1990). This sedimentary sequence rests nonconformably on the older metamorphic and igneous rocks, including the Vishnu Schist and Zoroaster Granite.

In the type section at Basalt Canyon (Hendricks, 1989; Hendricks & Lucchitta, 1974) the Cardenas Basalt consists of a 100-m-thick lower member composed of about six, coarsely ophitic flows of olivine basalt which vary in thickness from about 3 to 25 m. Beds of siltstone and sandstone 1.5 to 3 m thick occur between some of the flows. All flows possess vesicular tops and bottoms and massive to columnar-jointed central portions. Typically this lower member is poorly exposed, weathering to spheroidal masses surrounded by granular debris. Before alteration, this medium-grained basalt was similar in texture and mineralogy to the sills and dikes, while petrologic and chemical data suggest to some that this lower member is a spilitic hyaloclastite which is the altered effusive
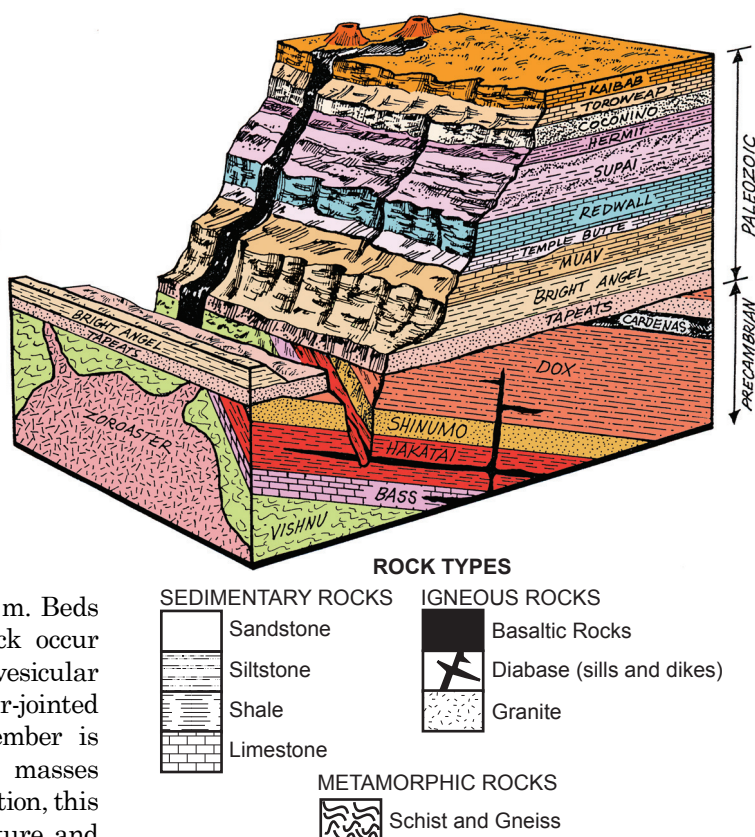

Figure 1. Stylized block diagram showing the stratigraphic position of Cardenas Basalt and Precambrian Diabase in the eastern Grand Canyon.
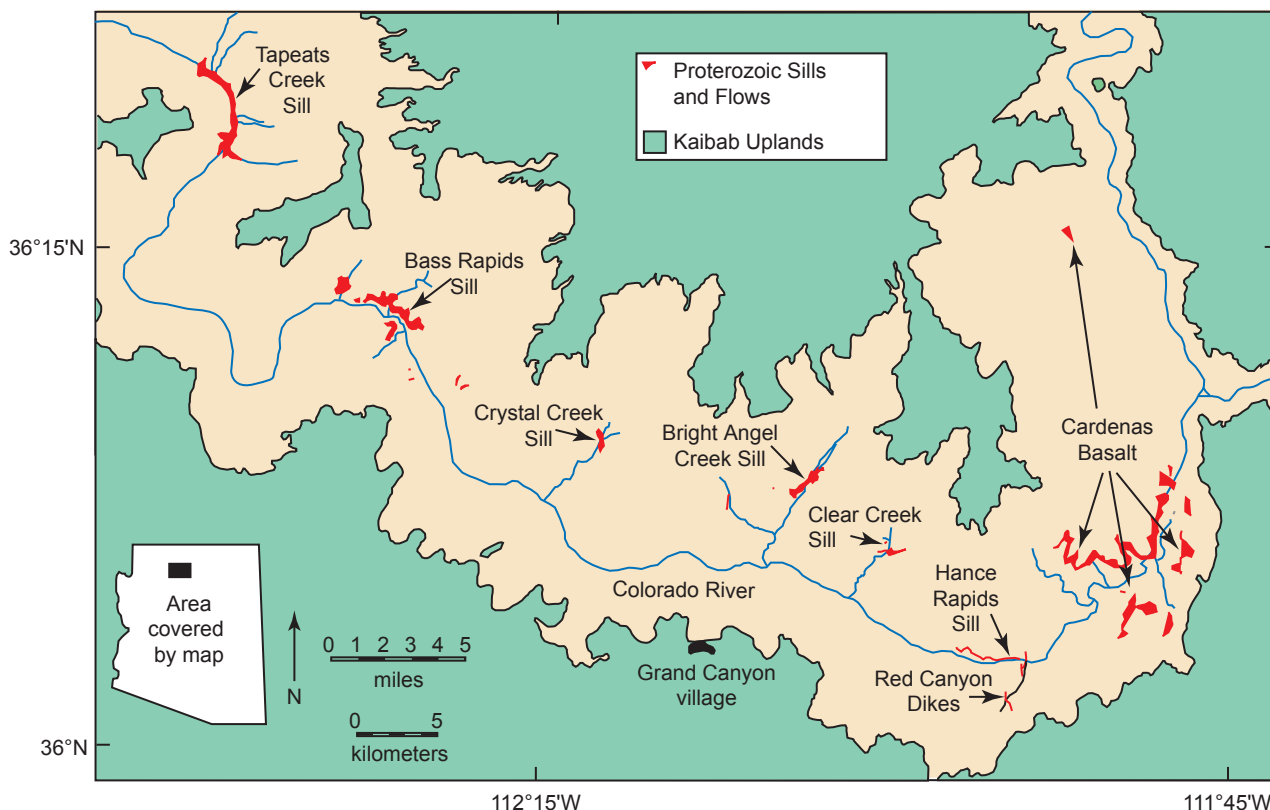

Figure 2. Location of Cardenas Basalt and Precambrian diabase in eastern Grand Canyon.

equivalent of those mafic intrusives (Lucchitta & Hendricks, 1983). However, the spheroidal masses may simply have resulted from onion-skin weathering rather than being suggestive of pillow structures, and therefore, the field evidence could indicate subaerial extrusion of these lower member basalts in a series of low-viscosity pahoehoe flows.

In contrast, the 200-m-thick upper member of the Cardenas Basalt comprises four to six, aphyric, intersertal to intergranular flows that change sequentially from basaltic andesite to basalt and then back to basaltic andesite upward through the section. The dramatic change to the resistant, finer-grained flows of the upper member coincides with the abrupt change in magma chemistry. Individual flows vary in thickness from about 20 to 50 m, each flow being separated from adjacent flows by laterally persistent siltstone and sandstone beds which generally range in thickness from 0.3 to 3 m. Amygdaloidal zones, from 2 to 5 m thick, are common near the bases and tops of the flows; scoriaceous flow breccia is conspicuous at the tops of several of them. Some of the flows exhibit crude columnar jointing in their middle to upper portions, whereas none of the flows exhibits any evidence of interaction with water.

The sills are not found in direct association with the Cardenas Basalt, but are confined to the lower part of the Unkar Group, particularly near the boundary between the Bass Formation and the Hakatai Shale, while the related dikes are intruded above the sills along faults that predate or are contemporaneous with the sills. These mafic sills crop out in seven locations along a 70–80 km length of the Grand Canyon (Figure 2) and range in thickness from 23 to 300 m. They are composed chiefly of medium-grained ophitic diabase. The dikes have a similar composition but are finer grained, as are the chilled margins of the sills. Early differentiation and crystal settling in the sills is evidenced by granophyre layers up to 10-m thick and felsite dikes, and by olivine-rich layers. The relationship of these intrusives to the Cardenas flows remains obscure because direct feeders to the flows and sills have never been recognized.

Sample Selection for K-Ar Analysis

The published geologic literature contains seven K-Ar analyses of Cardenas Basalt and two K-Ar analyses of Precambrian diabase (Elston & McKee, 1982; Ford, Breed, & Mitchell, 1972; Larson, Patterson, & Mutschler, 1994; McKee & Noble, 1974, 1976). Descriptions of these rocks are found in the Appendix of this paper and the K-Ar data have been collected into Table 1. General locations are shown in Figure 2.

Our goal was to more than double the K-Ar data for these Precambrian rocks of Grand Canyon, allowing a better and more comprehensive interpretation of K-Ar "ages." Thus, collection of new samples of Cardenas Basalt and Precambrian diabase had three purposes:

1. to complement and enlarge the published isotopic data set by sampling basalt and diabase in areas or stratigraphic levels not already described,
2. to select a variety of rock types, especially those with different potassium concentrations, in order to illustrate the variation of argon as a function of potassium,
3. to maintain precise geographic and stratigraphic data on samples so that double-checking and further sampling could be conducted.

Complete location data for the nine published K-Ar analyses and the 13 new analyses are found in the Appendix. The new K-Ar data have been combined with the published data into Table 1. Of the 13 new analyses, eight are from Cardenas Basalt and five are from Precambrian diabase.

A total of 19 new samples of Cardenas Basalt were collected. All new samples, except two, are from Basalt Canyon, one of the best and most studied outcrops. The Basalt Canyon section has poor exposure of the lower third of the Cardenas Basalt, so we collected two samples from the superior exposure of the lower 50 m at Lava Chuar Canyon. A split from each sample was submitted for 66 element geochemical analysis, and a slab was retained for thin-section petrographic analysis. The geochemical and petrographic data were used to evaluate each sample for its suitability for K-Ar analysis. We found an extreme variation in potassium in our new samples of Cardenas Basalt from 2.1% K_2O to 10.4% K_2O by weight. There was also a significant variation in silica (46.6 to 57.8% by weight SiO_2). Eight samples were selected for K-Ar analyses, including seven from Basalt Canyon (samples A:C-1, A:C-2, A:C-7, A:C-10, A:C-13, A:C-16, and A:C-19) and one from Lava Chuar Canyon (sample A:C-14).

Eleven new samples of Precambrian diabase were collected. Each sample was submitted for 66 element geochemical analysis, and, after thin-section petrographic analysis, each was evaluated for its suitability for K-Ar analysis. Five diabase samples were selected for K-Ar analysis. Three samples (A:DI-7, A:DI-10, and A:DI-11) come from the very thick sill complex within the Hakatai Shale at Bass Canyon, including two samples of the high-potassium granophyre zone near the top and one sample of very low-potassium diabase near the base of the sill. One sample (A:DI-9) is from the sill within the Bass Formation at Hance Rapids, and represents a whole-rock analysis of rock from which a pyroxene concentrate analysis has been published

Table 1. K-Ar data for Cardenas Basalt and Precambrian diabase of Grand Canyon. Thirteen samples coded with "A:" are new data collected and analyzed for this study. The other samples are from earlier publication. All samples are described in the Appendix.

Unit/Sample Code	K_2O (wt%)	^{40}K (ppm)	^{40}K (mol/g) x 10^{-8}	$^{40}Ar^*$ (ppm)	$^{40}Ar^*$ (mol/g) x 10^{-9}	$^{40}Ar^*$(%)	Total $^{40}Ar^*$ (ppm)	Total ^{40}Ar (mol/g) x 10^{-8}	^{36}Ar (ppm) x 10^{-5}	^{36}Ar (mol/g) x 10^{-13}	Model Age (Ma)	Uncertainty in Ma on age (1σ)
Cardenas FBM:(Bas)	2.40	2.377	5.95	0.1507	3.77	96.6	0.1559	3.90	1.6	4.50	853	15
Cardenas MN:b-8	3.10	3.070	7.68	0.1850	4.63	98	0.1886	4.72	1.2	3.20	820	20
Cardenas MN:Tb-8	3.33	3.298	8.25	0.1930	4.83	95	0.2050	5.08	3.1	8.60	800	20
Cardenas MN:b-4	4.185	4.1447	10.37	0.2390	5.98	99	0.2414	6.04	0.73	2.04	791	20
Cardenas EM:(Pal)	2.089	2.0689	5.18	0.1291	3.23	98	0.1319	3.30	0.80	2.23	843	34
Cardenas LPM:4D	1.231	1.469	3.05	0.1077	2.70	85.2	0.1263	3.16	5.7	15.7	957	35
Cardenas LPM:4E	1.282	1.269	3.18	0.10018	2.51	94.1	0.1063	2.66	1.9	5.18	1013	37
Cardenas A:C-1	4.005	3.965	9.923	0.2822	7.06	97.4	0.2897	7.25	2.3	6.37	935	19
Cardenas A:C-2	3.97	3.934	9.845	0.2448	6.13	97.1	0.2518	6.30	2.1	5.90	841	17
Cardenas A:C-7	0.782	0.775	1.94	0.05887	1.47	82.8	0.0711	1.78	3.7	10.4	984	24
Cardenas A:C-10	2.32	2.295	5.744	0.1049	2.62	94.3	0.1111	2.78	1.9	5.25	653	15
Cardenas A:C-13	7.43	7.355	18.41	0.2907	7.27	93.4	0.3109	7.78	6.2	17.1	577	12
Cardenas A:C-14	4.17	4.129	10.33	0.2023	5.06	95.2	0.2122	5.31	3.0	8.38	962	14
Cardenas A:C-16	10.5	10.398	26.02	0.4133	10.3	98.7	0.4196	10.5	1.9	5.34	580	12
Cardenas A:C-19	6.64	6.573	16.45	0.2878	7.20	97.7	0.2945	7.37	2.0	5.69	630	13
Diabase EM:(Han)	0.303	0.300	0.751	0.207	0.519	64.4	0.0322	0.806	3.5	9.71	914	40
Diabase EM:(Tap)	1.32	1.307	3.27	0.0955	2.39	92.5	1.1031	2.58	2.4	6.56	954	30
Diabase A:DI-5	2.002	1.982	4.96	0.1171	2.93	89.35	0.1311	3.281	4.3	11.88	806	18
Diabase A:DI-7	0.754	0.747	1.87	0.03893	0.974	80.0	0.0487	1.22	3.0	8.24	728	20
Diabase A:DI-9	1.51	1.496	3.74	0.07468	1.87	89.8	0.0832	2.08	2.6	7.18	703	15
Diabase A:DI-10	8.61	8.527	21.34	0.5737	14.36	96.4	0.5951	14.89	6.5	17.94	895	20
Diabase A:DI-11	8.245	8.166	20.43	0.4206	10.52	94.3	0.4460	11.16	7.8	21.66	721	14

for the sample we call EM:(Han). One new sample (A:DI-5) is from a dike within the Hakatai Shale at Red Canyon and probably represents the same intrusive event that formed the diabase sill at Hance Rapids.

Sample Preparation and Analysis

Two kilogram samples of rock were returned to the petrographic laboratory and sawed to remove exterior surfaces which could be contaminated. Thin-sawed samples of each rock were retained for thin-section petrographic analysis. Interior blocks each representative of the whole rock and each weighing about 1 kg were washed, dried, and then crushed in an iron mortar. After milling and grinding, the residue was sieved. The 80–200 mesh (0.18–0.075 mm) particles were retained for K-Ar analysis. The approximate 20-gram split of particles finer that 200 mesh was submitted for bulk geochemical analysis (the 66 element "MER" package by XRAL Laboratories of Don Mills, Ontario) and the remainder of the processed rock powder was archived with the intention of performing further isotopic analyses.

Potassium and argon were measured in the 13 new whole-rock samples by Geochron Laboratories of Cambridge, Massachusetts, under the direction of Richard Reesman, the K-Ar laboratory manager. The 13 preparations were submitted to Geochron Laboratories with the statement that each sample was a whole-rock preparation from igneous rock of general "basaltic" composition and that the lab should expect high argon concentration. The lab was not given any location or "age" information.

The analytical methods used for the nine published determinations for K-Ar appear to be comparable to our 13 new determinations. Comparability includes sample preparation, analytical technique and reporting. Two published whole-rock Cardenas analyses (LPM:4D and LPM:4E by Larsen, Patterson, & Mutschler, 1994) were also performed by Geochron Laboratories using the same equipment. Three Cardenas analyses (MN:b-8, MN:Tb-6, and MN:b-4) and two diabase analyses (EM:(Han) and EM:(Tap)) performed at the USGS lab also used flame photometry and the standard isotope-dilution technique with mass spectrometer. Also, samples FBM:(Bas) and EM:(Pal) had the same analytical technique. Therefore, we can say that the published K-Ar analyses, although performed at three or four different labs, show evidence of significant standardization in sample preparation, analytical method, and reporting.

The new analytical data as well as the published analytical data are reported in Table 1. For comparability we have converted the data to the same format. The concentration of K_2O (weight%) was measured by the flame photometry method, the reported value being the average of two readings from each sample. The ^{40}K concentration (ppm) was calculated from the terrestrial isotopic abundance using the concentration of K. The concentration in ppm of $^{40}Ar*$, the supposed "radiogenic argon," was derived by the conventional formula from isotope-dilution measurements on a mass spectrometer by correcting for the presence of atmospheric argon whose isotopic composition is known. The concentration of ^{36}Ar is also calculated from the ^{40}Ar and total Ar measurements.

Petrography and Chemistry

The original mineralogy of the Cardenas lavas was difficult to decipher upon petrographic examination of the collected samples due to their extensive alteration and some weathering effects. Nevertheless, estimates were made of each sample's original mineral composition, and these data are found in the Appendix. Some data on whole-rock chemistry are also included.

According to our estimates, our samples of the lower member flows appear to have originally consisted of 45–50 vol.% plagioclase, 20–25 vol.% augite, 15–18 vol.% olivine, 5–7 vol.% titanomagnetite and ilmenite, and 5–10 vol.% glass (mesostatis)/groundmass. Our apparent overestimates of the augite and olivine contents compared to those reported by Larsen, Patterson, & Mutschler (1994) are due to the difficulty of distinguishing the alteration products of augite and olivine from those of the originally glassy groundmass. Nevertheless, this mineral association and the subequant ophitic augite grains enclosing the plagioclase laths mean the rock is appropriately classified as an olivine basalt.

The post-extrusion alteration of all lower member flows is similar. The late-stage glassy groundmass has been altered to chlorite, epidote and/or red-brown clay, olivine has been completely replaced by chlorite, clay, and hematite, plagioclase has been largely altered to saussurite and/or replaced by fine-grained sericite, chlorite, and clay, and augite has generally only sustained minimal replacement by chlorite, clay, and hematite. Chlorite, calcite, and quartz (mostly chalcedony) commonly form amygdules and vein fillings.

Whereas it could be expected that this alteration may have changed the original rock chemistry, Larsen et al. (1994) used an isochron plot to show that these rocks have probably undergone minimal enrichment or depletion of individual major-element oxides during hydration. However, because of the abundant clay alteration, the loss on ignition (loss at 1000°C after samples initially dried to constant weight) varies between 4 and

10 wt%, which is almost exclusively attributable to water loss. Otherwise, the variable contents of CaO (4.0–6.5 wt%), Na_2O (0.5–4.5 wt%) and K_2O (2.0–7.5 wt%) are due to the alteration mineralogy, while the relatively high total iron-oxide content (FeO *plus* Fe_2O_3 analyses recalculated to give a total expressed as *FeO) averaging 10 wt% suggests a tholeiite, and the average 16.5 wt% Al_2O_3 is compatible with a high-alumina basalt of shoshonitic affinities.

The pronounced rock-type variations of the upper member flows are reflected in the wider ranges in the estimated original mineral compositions— 45–60 vol.% plagioclase, 20–30 vol.% augite, 5–18 vol.% olivine, 2–5 vol.% titanomagnetite and ilmenite, and 7–15 vol.% glass (mesostasis)/groundmass. Larsen et al. (1994) reported the sporadic occurrence of pigeonite, and because of the aphyric texture and lower olivine content suggested all the flows can be classified as tholeiitic olivine basalts or basaltic andesites.

The variable chemical alteration of the upper member flows is generally similar to that of the lower member flows, but is often less extensive. Again the style and mineralogy of the alteration is reflected in the major-element oxide contents in whole-rock analyses, but the loss on ignition attributable to water loss at 2.0–3.5 wt% is consistently much lower than that of the lower member flows, indicative of the alteration being less extensive. Both Al_2O_3 and total iron-oxide content (as *FeO) are relatively uniform in all samples, Al_2O_3 averaging about 14.4 wt% and *FeO about 12.9 wt%, with the exception of A:C-19 with 20.1 wt% *FeO. Samples A:C-16 and A:C-19 with 10.4 wt% and 8.1 wt% K_2O respectively, compared to the 3 wt% K_2O average of the other samples, are heavily altered, but they also only contain trace CaO and Na_2O compared with the 4.3 wt% CaO and 3.5 wt% Na_2O averages in the other samples.

Larsen et al. (1994) concluded that some of these chemical variations between the upper member flows appear to be related to initial differences in magma composition. They found that K_2O increased abruptly in the top two flows, while CaO decreased abruptly (A:C-19 is our sample from the top flow). However, our samples do not follow all the chemical trends they observed in their samples, which again emphasizes the complexity of the interplay between original magma compositions and subsequent alteration during and after lava cooling. Nevertheless, it is possible to conclude from the major-element oxide analyses of these rocks that they are tholeiitic, varying from quartz tholeiites to tholeiitic andesites (Yoder & Tilley, 1962).

The intrusive rocks of the sills and dikes are all diabases, except for the granophyres found segregated by differentiation at the tops of some of the thicker sills (for example, the sill at Bass Canyon). Mineralogically, with 45 vol.% plagioclase, the diabases are similar to the lower member flows, and they are also ophitic. However, the main observable difference between the lower member flows and these mafic intrusives is in the color of the augite in thin section, which is in turn due to differences in the TiO_2 content of the augite Larsen et al. (1994). Chemically, the mafic intrusives exhibit similarities with the lower member flows, but there are also dissimilarities Larsen et al. The diabases have not suffered alteration as intense as that in the lower member flows (nor of that in the upper member flows), and what minor alteration there is, is primarily sericite and chlorite. The granophyre is distinctive in outcrop due to its felsic character, marked by 20–25 vol.% quartz, 8–10 vol.% orthoclase, and 5–10 vol.% biotite.

Previous workers appear to have created a conundrum in their interpretation of K-Ar dating of these basalts and diabases. By accepting the Rb-Sr system as an isochron, they have argued that the original rubidium in these rocks has been a closed system, a major assumption for a valid Rb-Sr isochron. The observation of the strong linearity of Rb-Sr plots, indeed, is an argument for a closed system for rubidium in these rocks as pointed out by Larsen et al. (1994). However, potassium is an alkali element very similar geochemically to rubidium, and the argument, by its association, makes potassium in these basalts and diabases a closed system as well. Workers (Elston & McKee, 1982; Larsen et al.) who have accepted the Rb-Sr isochron have not argued, for example, that potassium has been added to these basalts and diabases during the hydration process which altered mineral phases within these rocks. Metasomatic addition of potassium could explain younger-than-expected ages. That has not been argued, and apparently for good reason. Instead, previous workers have questioned only the retention of argon by these rocks. Accepting an "argon loss model" for these rocks, however, as we point out below, raises many inconsistencies and questions. Hence, the creation of a conundrum. Although we agree that a strong case can be made against using the K-Ar system to date these rocks, the concentration and isotopic abundances of argon in these rocks needs to be explained by an adequate model.

Results

K-Ar model "ages" for each of the 22 analyses are listed in Table 1. These model ages are calculated by the standard equation of Dalrymple & Lanphere (1969) using the mole ratio of $^{40}Ar*$ to ^{40}K, both abundances being listed in Table 1. The model age method assumes no radiogenic ^{40}Ar was present when diabase and lavas

cooled to form rocks. For the Cardenas Basalt the K-Ar model "ages" range from 577±12 Ma (million years with 1σ error) to 1013±37 Ma, with the mean age of 816 Ma (n=15). For the Precambrian diabase the model "ages" range from 703±15 Ma to 954±30 Ma, with the mean age of 817 Ma (n=7). Although the mean ages for Cardenas Basalt and Precambrian diabase are essentially the same (816 Ma), the wide variation in model ages remains unexplained. Ages for Cardenas Basalt are not as predicted by superposition (that is, relative positions in the succession of lava flows). For example, sample A: C-13 from the base of the Basalt Canyon section is, therefore, the oldest of the Cardenas samples according to superposition of the lava flows. Yet, A:C-13 gives the *youngest* age of all of the 15 Cardenas samples (577 Ma). Sample LPM:4E comes from near the top of the Cardenas Basalt at about 220 m above the base, and, therefore, is one of the youngest flows according to superposition. Yet, LPM:4E gives the *oldest* age of 1013±37 Ma. Also, discordant model ages were obtained for the granophyre zone near the top of the sill at Bass Rapids: 895±20 Ma and 721±14 Ma (diabase samples A:DI-10 and A:DI-11 respectively). The geologic observations at Bass Rapids require that the granophyre zone represents a single cooling unit at the top of the sill and the two samples are separated by only a few meters. Furthermore, for the Hance Rapids diabase sill, pyroxene mineral concentrate sample EM:(Han) gave a model age of 914±40 Ma, whereas the whole-rock sample A:DI-9 from the same sill gave 703±15 Ma.

Figure 3 is the ^{40}Ar versus ^{40}K graph for Cardenas Basalt. We plot the data with 2σ estimated error bars. A strong linear trend is apparent which appears to represent an isochron. The two-error
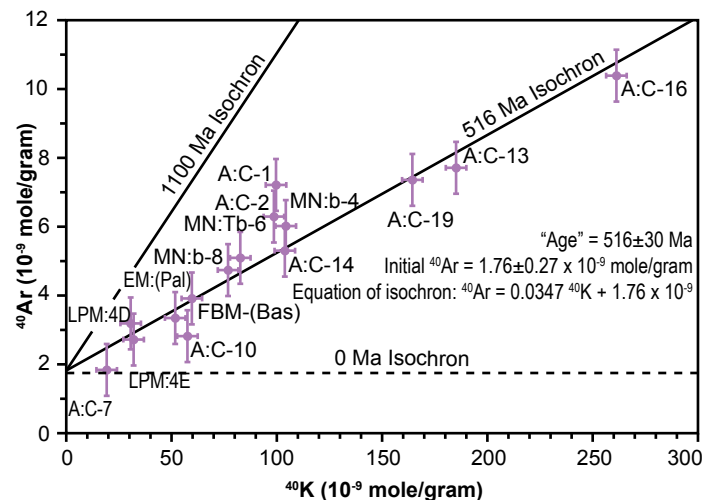

Figure 4. ^{40}Ar versus ^{40}K for Precambrian diabase. "Isochron" and "age" calculated from all seven data points. Bars represent 2σ uncertainties.

Figure 3. ^{40}Ar versus ^{40}K for Cardenas Basalt. "Isochron" and "age" calculated from 14 of 15 samples. One sample data point (A:C-1) was not included in the isochron calculation. Bars represent 2σ uncertainties.
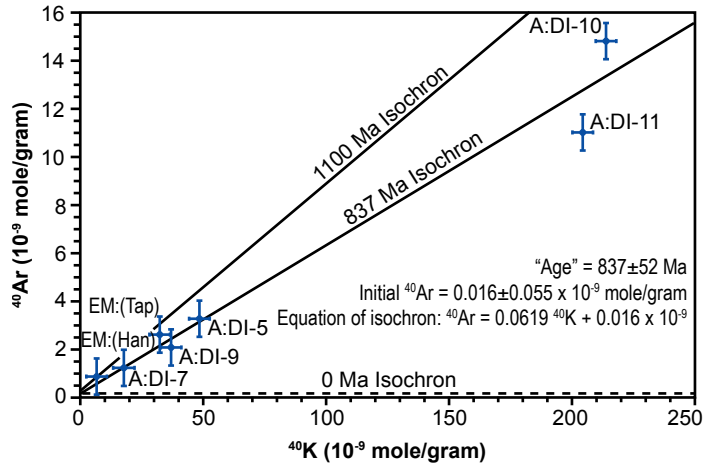
regression method of York (1969) was used to fit the line to the data. Of the 15 points, only one (A:C-1) was recognized by the computer operation to lie significantly off the line, and that sample was not included in the regression calculation. The equation of the line is shown in Figure 3 and is plotted. There is a significantly non-zero ^{40}Ar value for zero ^{40}K, which would appear to refute the zero ^{40}Ar* assumption of the model age technique. The computer calculated ^{40}Ar initial is 1.76±0.27×10^{-9} mole/gram (2σ error). The slope of that line was used to calculate the isochron "age" of 516±30 Ma (2σ error).

Figure 3 also includes the 1100 Ma reference isochron which is widely assumed to be the true age of Cardenas Basalt based on the Rb-Sr isochron (McKee & Noble, 1974). The ^{40}Ar-^{40}K data plot significantly *beneath* what would be expected for 1100 Ma age and have significantly *lower slope* than what would be expected for 1100 Ma age.

Figure 4 is the ^{40}Ar versus ^{40}K graph for Precambrian diabase. Two-sigma error bars and the best fit two-error regression line (York, 1969) are plotted. All seven data points are accepted by our computer model in plotting the line, the slope of which is most strongly affected by the two high-potassium grano-phyre samples (A:DI-10 and A:DI-11). A very small, essentially zero, value for initial ^{40}Ar is calculated and the isochron age is 837±52 Ma (2σ error). The 1100 Ma reference isochron shows the discordance with the 1100 Ma Rb-Sr isochron age.

Figures 5 and 6 are the ^{40}Ar/^{36}Ar versus ^{40}K/^{36}Ar graphs for Cardenas Basalt and Precambrian diabase. Significant analytical error builds up in the measurement of the abundance of ^{36}Ar as the ratio of ^{40}Ar to ^{36}Ar increases. That is why data points in the upper right of Figures 5 and 6 have large error bars.
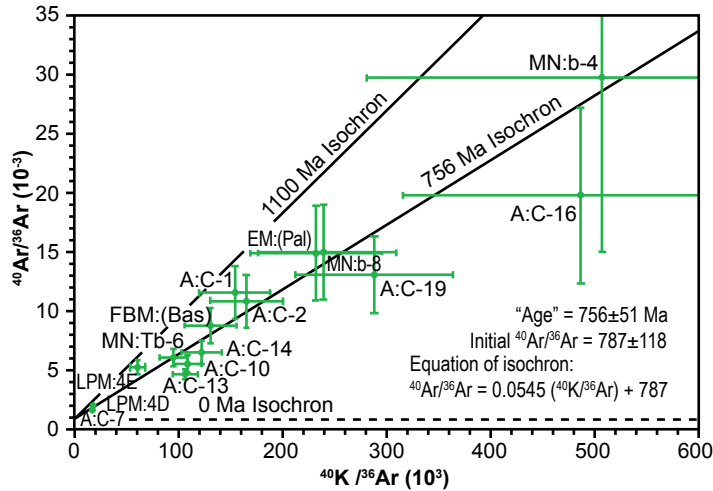
Figure 5. $^{40}Ar/^{36}Ar$ versus $^{40}K/^{36}Ar$ for Cardenas Basalt. "Isochron" and "age" calculated from fourteen of fifteen data points. Data point A:C-13 was not included in the isochron calculation. Bars represent 2σ uncertainties.

Even considering these larger errors, linear trends are apparent. The two-error regression method is used to plot lines in Figures 5 and 6. For the $^{40}Ar/^{36}Ar$ versus $^{40}K/^{36}Ar$ plot in Figure 5 for Cardenas Basalt the isochron age is 756 ± 51 Ma. Most important is the y-intercept indicating significant initial $^{40}Ar/^{36}Ar = 787\pm118$ (2σ) which is 2.7 times higher than $^{40}Ar/^{36}Ar = 295.5$, the present atmospheric value. This argues that a major part of the ^{36}Ar is not atmospheric contamination but was included in the rocks when they formed. The associated diabase of Figure 6 gives a linear array with an isochron age of 676 ± 35 Ma and initial $^{40}Ar/^{36}Ar$ about 1.5 times the modern atmosphere. In each case the calculated K-Ar isochron age is significantly less than the generally accepted Rb-Sr isochron age of 1100 Ma.
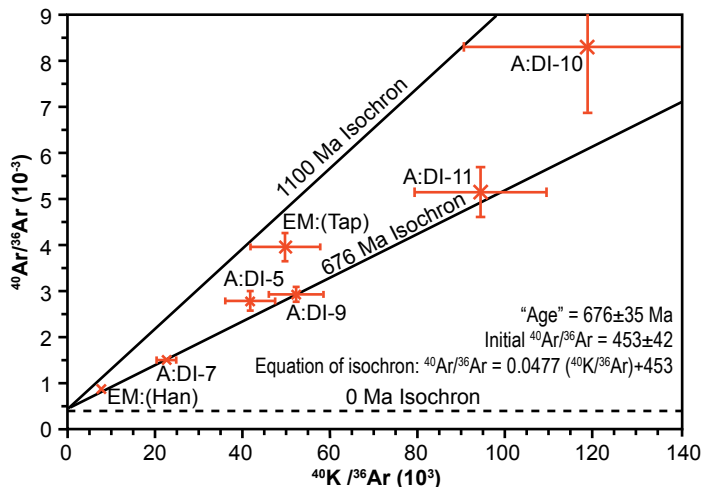

Figure 6. $^{40}Ar/^{36}Ar$ versus $^{40}K/^{36}Ar$ for Precambrian diabase. "Isochron" and "age" calculated from six of seven data points. Data point EM:(Tap) was not included in the isochron calculation. Bars represent 2σ uncertainties.

Discussion of Discordant "Ages"

Why does the K-Ar data yield significantly younger ages for Cardenas Basalt and Precambrian diabase than the Rb-Sr data? Five explanations should be considered.

1. Argon Reset Model

When McKee & Noble (1976) published their Rb-Sr isochron age of 1070 Ma (recalculated with new Rb decay constant) for Cardenas Basalt, they explained the four K-Ar model ages (819±20, 809±20, 790±20, and 843±34 Ma) available to them as caused by resetting during an episode of heating about 800 Ma ago. They assumed that a significant quantity of ^{40}Ar was released by metamorphism. When another Cardenas K-Ar model age became available (855±15 Ma), Elston & McKee (1982) reiterated this interpretation specifying the Cardenas heating event at 823±26 Ma. Elston & McKee argued from three new diabase model ages (913±40, 954±30. and 904±100 Ma) that another earlier heating event reset diabase ages at 930±25 Ma when the diabase was more deeply buried than Cardenas Basalt.

Figure 7 shows how the reset model would interpret the linear arrays of ^{40}Ar versus ^{40}K and $^{40}Ar/^{36}Ar$ versus $^{40}K/^{36}Ar$ for our larger data set of Cardenas Basalt. Because the reset model assumes the Cardenas Basalt has an age of 1100 Ma, a large quantity of ^{40}Ar must be removed from these rocks to explain why they have only half the argon expected. Figure 7 shows how a heating event at 516 Ma (584 million years after the eruption of the Cardenas Basalt) removed almost all of the early-formed argon essentially resetting the isochron to zero age making, then, a horizontal linear array. The passage of 516 Ma since the heating event allowed the present buildup of ^{40}Ar by decay of ^{40}K.

Figure 7 shows sample A:C-16 on today's linear array at point C′. However, 1100 Ma ago (slightly less than one half-life of ^{40}K) sample A:C-16 had nearly twice its present quantity of ^{40}K (approximately 480×10^{-9} mole/gram) and a very low quantity of argon (most of the argon is assumed to have vented as the lava flows cooled). Argon buildup should have moved the sample to point C on the 1100 Ma isochron. The postulated heating event deflected sample A:C-16 when it had an age of 584 Ma (516 Ma ago) from point B (on the 584 Ma isochron) to point B′ (on the 0 Ma isochron) as 14×10^{-9} mole/gram of ^{40}Ar and a significant quantity of ^{36}Ar were lost. During the 516 Ma since the heating event, sample A:C-16 moved from point B′ (on the 0 Ma reset isochron) to point C′ (on the 516 Ma

isochron). Other samples of Cardenas Basalt followed similar trajectories on the ^{40}Ar versus ^{40}K and $^{40}Ar/^{36}Ar$ versus $^{40}K/^{36}Ar$ graphs leaving the linear array suggesting an isochron age of 516±30Ma.

Our larger data set shows that the heating event postulated by McKee & Noble (1976) and Elston & McKee (1982) could not have reset the Cardenas Basalt K-Ar system 823±26Ma ago. Our new data

set which forms the 14-point linear array does two things:

1. it invalidates the zero initial argon assumption of the K-Ar model ages; and
2. it specifies the heating event at 516±30Ma ago if a reset model is to be imposed on the data.

However, an age of 516±30Ma is Upper Cambrian, not Proterozoic. The conventional interpretation of Grand Canyon Upper Cambrian stratigraphy at Basalt Canyon is that the Tapeats Sandstone (Upper Cambrian) was sitting level on the floor of an ocean

just above the Great Unconformity and just a few hundred meters above 12° dipping Cardenas Basalt. No trace of the assumed Upper Cambrian heating event is seen in the Tapeats Sandstone at Basalt Canyon. Therefore, the reset model has incorrect timing and fails to explain the K-Ar data within conventional geology.

2. Argon Leakage Model

Could continuous argon leakage during the history of Cardenas Basalt and Precambrian diabase explain why these rocks have lost almost half of their ^{40}Ar which would be expected to build up in 1100Ma? Larson et al. (1994) defended prolonged burial metamorphism to explain loss of argon in Cardenas Basalt. For seven K-Ar dates from Cardenas Basalt, they observed a negative correlation between the abundance of potassium and the K-Ar model age. All 22 samples are plotted in the K-Ar model age versus K_2O graph in Figure 8. Negative correlation within Cardenas Basalt is apparent, a trend that is not as strong within the diabase. Our increased data set shows that the three highest-potassium samples of Cardenas Basalt (A:C-13, A:C-16, and A:C-19) do, indeed, have the lowest K-Ar model ages. Larson et al. interpreted this trend as indicative of higher burial alteration of glassy and aphanitic (mesostasis) material in the more-felsic, higher-viscosity, higher-potassium flows.

Figure 9 depicts the continuous argon leakage model for Cardenas Basalt. Samples should be positioned on the 1100Ma isochron, but, according to the leakage model, because of diffusion of argon out of glassy and crystalline material, are positioned on the 516Ma isochron. The model leads to a rather remarkable explanation—the idea of a "leakage isochron." The explanation appears remarkable because leakage would be thought of as a random process, not as a process so strongly correlated with the abundance of potassium.

Sample A:C-16 in Figure 9 illustrates the argon leakage model. That sample sits at point C′ today, but, according to the leakage model, was at point A about 1100Ma ago. Originally, sample A:C-16, and all the other Cardenas samples, had almost twice the quantity of ^{40}K than today. According to the leakage model, continuous argon loss occurred as sample A:C-16 moved away from its original position at or near point A. After 584Ma passed (at 516Ma), the sample should have been at point B. Instead of moving through point B to point C, argon diffusion deflected the trajectory through point B′ to C′. Other samples should have followed similar trajectories, but
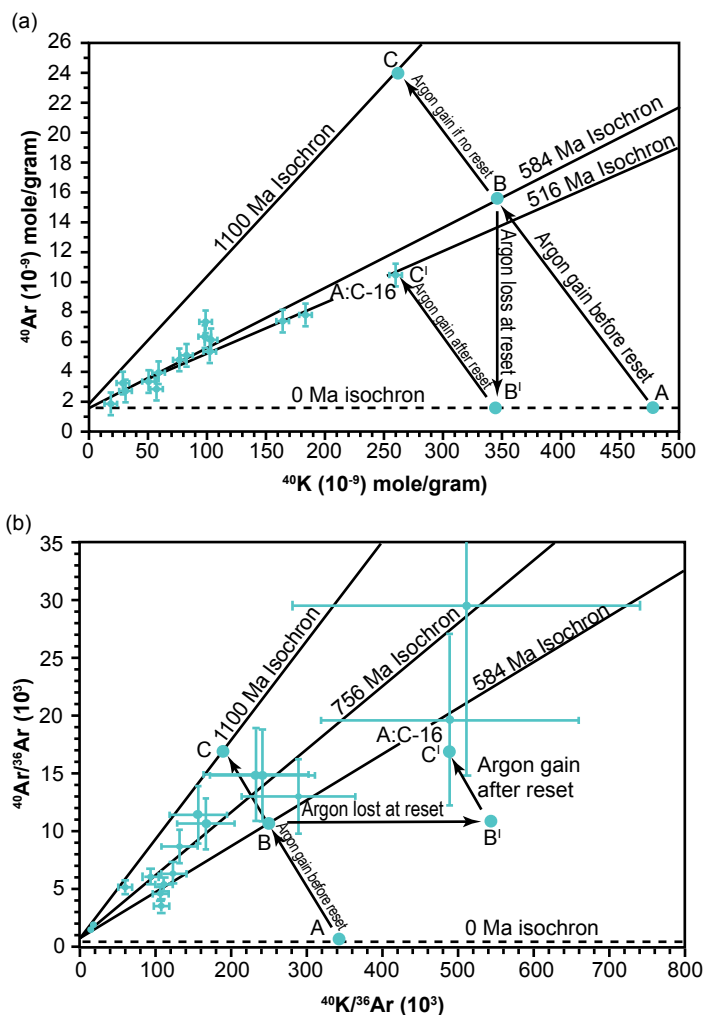
Figure 7. Diagrams illustrating the "argon reset model" for Cardenas Basalt. The two diagrams follow sample A:C-16 through the postulated metamorphic event which allows removal of about half of the sample's argon. Other samples on the diagrams would follow similar pathways.
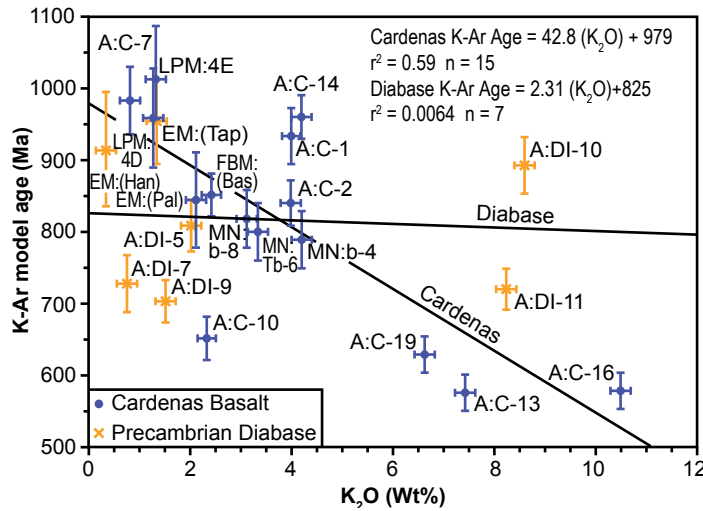
Figure 8. K-Ar model age versus K_2O for Cardenas Basalt and Precambrian diabase. Bars represent 2σ uncertainties.

with significantly less argon loss. To make the 516 Ma isochron by such a process requires an extraordinary correlation between the quantity of argon leakage and the quantity of potassium. Because Cardenas Basalt differs widely in its abundance of potassium, Elston & McKee (1982) rejected the continuous leakage model:

> Slow leakage would have had to occur in the exact proportions in both the minerals and the whole rock to produce the similar ages—an unlikely situation.

Because ^{36}Ar is nonradiogenic, we can use it as a tracer to test any model which requires significant leakage of ^{40}Ar. The two isotopes have similar mass and nearly identical chemical properties. Diffusion should not select one isotope over the other. Two requirements of the leakage model are:

1. the rocks must have had significant ^{36}Ar originally, and
2. there must have been significant ^{36}Ar loss by leakage, especially high leakage in the rocks with high potassium.

Figure 9b illustrates the need for significant initial ^{36}Ar and the requirement for significant ^{36}Ar leakage. In order for high-potassium sample A:C-16 to acquire its present $^{40}K/^{36}Ar$ of 5×10^5 according to the leakage model, it has to begin near point A in Figure 9b with $^{40}K/^{36}Ar$ of about 4×10^5. This is a significant quantity of initial ^{36}Ar, and about 45% of it appears to have been lost by leakage during 1100 Ma of ^{40}K decay to move the sample to its present position at point C′ in Figure 9b. If significantly less ^{36}Ar was present initially and sample A:C-16 began near point D in Figure 9b, leakage would deflect that sample's argon and potassium composition toward point F′, very different from its proper

position at C′. Other samples of basalt and diabase could be used to illustrate the above conclusion about high initial ^{36}Ar and significant ^{36}Ar loss that the leakage model requires. Rocks with the highest ^{40}K should have experienced the highest ^{36}Ar loss.

Is there a strong negative correlation between the abundances of ^{36}Ar and ^{40}K in Cardenas Basalt and Precambrian diabase as the leakage model would require? Figure 10 is the plot of the present abundances of ^{36}Ar and ^{40}K in the 22 Grand Canyon samples. Linear regression indicates lines in Figure 10 possessing *positive* slopes, not *negative* slopes. The two high-potassium Cardenas Basalt samples (A:C-16 and A:C-13) have *more, not less*, ^{36}Ar than the average of the low-potassium Cardenas samples. The two high-potassium granophyres (A: DI-10 and A:DI-11) have the highest ^{36}Ar (and highest ^{40}Ar) of
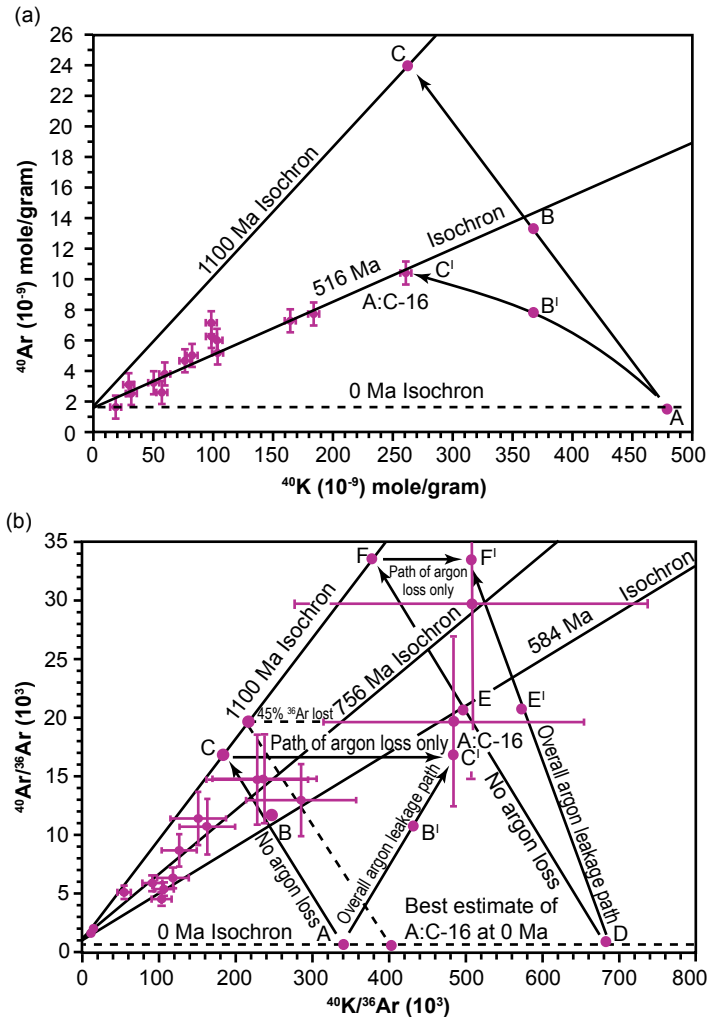

Figure 9. Diagrams illustrating the "argon leakage model" for the Cardenas Basalt. The two diagrams follow sample A:C-16 through continuous argon leakage which is postulated to remove about half of the sample's argon. Other samples follow similar pathways.
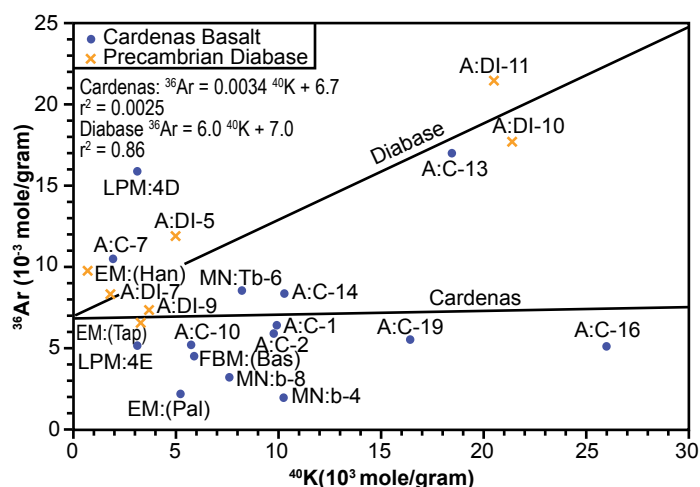
Figure 10. ^{36}Ar versus ^{40}K for Cardenas Basalt and Precambrian diabase. Note that non-negative correlation lines argue that the high-potassium samples (also high ^{40}Ar) have not lost significantly more ^{36}Ar. Positive correlation appears to fail a requirement of argon loss models.

all twenty-two samples. Why would high-potassium granophyre, which supposedly experienced very significant argon leakage, retain so much ^{36}Ar? These data do not fit well with the continuous argon leakage model.

3. Argon Inheritance Model

An alternate model to the above two argon-loss models can be called the inheritance model. We could suppose that Precambrian magmas of Grand Canyon had differing potassium concentrations and that those magmas with higher potassium had higher partial pressures of argon. Furthermore, we might suppose that these Precambrian magmas did not vent completely their argon. By this mechanism high-potassium magmas would create lava flows and sills possessing higher argon, and a linear array could characterize the ^{40}Ar versus ^{40}K plot. By this mechanism the argon of Grand Canyon igneous rocks would have been largely inherited from its pre-existent source. The model may explain the linear-array plots of data such as Figures 3, 4, 5, 6, and 8.

Although a strong case can be made that some of the argon is inherited, the extreme argon variation within a single sill is not well explained. Why would the two high-potassium granophyre samples (A:DI-10 and A:DI-11) have about ten times more ^{40}Ar than the single sample of normal diabase (A:DI-7)? All three samples come from what seems to be the same diabase sill at Bass Rapids, and would seem to require the same magma source. Therefore, the argument for inheritance of major argon might appear weak.

Nevertheless, there are numerous examples in the relevant literature of excess argon that has thus been inherited (Dalrymple & Lanphere, 1969), including the 1986 lava dome at Mount St. Helens (Washington, USA) (Austin, 1996) and recent lava flows at Mt. Ngauruhoe (North Island, New Zealand) [*Snelling,* 1998]. Admittedly, these known examples of inheritance are usually modern or recent volcanic rocks and usually only involve a couple of hundred thousand years of radiometric age, but this is thus suggestive of the possibility of inheritance in ancient volcanic rocks, such as these in Grand Canyon.

In spite of the doubts already expressed, it is still possible that excess argon may have been inherited by the Cardenas Basalt flows and the mafic intrusives. Thus some of the variation in K-Ar model ages between the different flows, sills, and dikes could be attributable to both differing amounts of excess argon in the magma over the duration of this igneous activity, and to how much excess argon was degassed from the cooling rocks and how much retained. In the case of the diabase sill at Bass Rapids, this might also explain why there is ten times more ^{40}Ar in the granophyre than in the normal diabase—just as differentiation separated the "lighter" felsic minerals to the top of the sill to form the granophyre, so too the inherited ^{40}Ar diffused upwards during cooling of the sill to concentrate also in the granophyre.

4. Argon Mixing Model

An alternate model similar to the inheritance model involves mixing of two different kinds of magmas. Rather than inheritance of potassium and argon from numerous different magma types, we could suppose only two original types of magma. The first magma we could suppose was like sample A:DI-7 with low potassium and low argon, whereas the second magma we could suppose was like sample A:C-16 with very high potassium and very high argon. Because the two magma end-members display a ten-fold difference in potassium and argon, the combination of different proportions of these two magmas could produce the various concentrations of potassium and argon we have today in the basalt and diabase. Furthermore, the mixing process of various proportions of the two magmas would produce a linear pattern or "mixing line" on a graph of ^{40}Ar versus ^{40}K (that is, Figure 3). For example, a magma mixed with a significant quantity of A:C-16 would lie on the line between A:DI-7 and A:C-16, but nearer A:C-16. Another magma formed mostly of A:DI-7 would also lie on the line between the two end-members, but closer to A:DI-7. That "mixing line" would be identical to an "isochron" but have absolutely no "age" significance.

Two observations appear to be fatal to the argon mixing model. First, the single diabase sill at Bass

Rapids would have to reflect the character of essentially two unmixed magmas. The high-argon granophyre at the top of the sill could not be differentiated by gravitational removal of mafic minerals (the conventional interpretation of granophyre), but would have to be a completely different type of magma within the sill. How could two types of magma be intruded into a narrow fracture, presumably during a single catastrophic event, but retain their original chemical identities by not mixing? This is a significant problem for both the inheritance and mixing models.

The second problem for the mixing model involves other major and trace elements. If the concentrations of potassium and argon in diabase and basalt are controlled by a binary mixing process, then the other elements should reflect the mixing process as well. Samples A:DI-7 and A:C-16 should be end-members of other mixing lines besides potassium and argon. However, analysis of the geochemical data does not produce other-element mixing lines with A:DI-7 and A:C-16 as obvious end-members. The two-component mixing model does not fit the geochemical data in a convincing way.

5. Change of Decay Model

Discordance between Rb-Sr and K-Ar dating methods for Grand Canyon Precambrian rocks has led many geologists to propose some very speculative models suggesting significant argon loss. These argon loss models, either by reset event or continuous leakage, have significant problems explaining the data. These difficulties arise because the basalt and diabase are interpreted within an evolutionary context with the assumption of constancy of radioisotope decay. Could the discordant ages be better interpreted if a singularity disrupted normal radioactive decay sometime in the past? Could ^{87}Rb decay and/or ^{40}K decay constants be altered to make the data be interpreted in a concordant way? The mathematics simply requires a change to one or both decay constants and they could be concordant. The important question remains as to how the physics of such non-constant decay could occur. One intriguing explanation is that both ^{87}Rb and ^{40}K decay were accelerated in the past, and that ^{87}Rb decay was accelerated more than ^{40}K decay. We might imagine the physics of the acceleration of the decay process is mass dependent, with β-decay of more-massive ^{87}Rb having occurred *faster* than β-decay of less-massive ^{40}K. This explanation, with appropriate increases in the decay "constants" of ^{87}Rb and ^{40}K, could bring the two radioisotope clocks into concordance. This model would have application in explaining other discordances between Rb-Sr and K-Ar data where the K-Ar "age" is much younger than the Rb-Sr "age."

Other Considerations

The negative correlation between the abundance of K_2O and the K-Ar model ages was initially observed by Larson et al. (1994). The seven samples they found were strongly correlated, and all came from the Cardenas Basalt upper member flows. If, therefore, the samples from the lower member flows (A:C-10, A:C-13, and A:C-14) are ignored in the graph in Figure 8, then the negative correlation of K-Ar model age with K_2O abundance is quite pronounced (A:C-10 and A:C-14 are clearly outriders). This relationship thus needs to be explained, as does the poor correlation in the Cardenas Basalt lower member flows and the mafic intrusives.

The abundance of K_2O is, of course, related to the mineral compositions of these mafic rocks. In the granophyre, the major K_2O-bearing minerals are orthoclase and biotite, whereas in the basalts and diabases neither augite nor olivine has any K_2O in it, the only major mineral constituent with more than a trace of K_2O being plagioclase. This only leaves the glassy mesostasis/groundmass as potentially the primary bearer of the K_2O contents of these mafic rocks. It represents the last-crystallized material or the "dregs" of cooling/crystallization, probably being quite felsic and thus high in silica and alkalis. However, the highest K_2O contents in our samples do not correlate with the highest volume percentage of glassy mesostasis/groundmass (see Appendix).

The other possibility is that the K_2O contents reside in the alteration mineralogy, but sericite is the only likely candidate, being consistently present as one of the alteration products of plagioclase. On the other hand, the glassy mesostasis/groundmass is often altered to chlorite, epidote, and clay, none of which contain more than trace amounts of K_2O, unless the clay were illite. As already noted, the highest-K_2O samples in our Cardenas Basalt data set (A:C-13, A:C-16 and A:C-19) have the lowest K-Ar model ages, but these samples are not necessarily all the most intensely altered. Yet the two granophyre samples (A:DI-10 and A:DI-11) have equally high K_2O contents and yield higher K-Ar model ages, though one of them has a virtually identical K-Ar model age to the diabase (A:DI-7) beneath it in the same sill, even though the diabase only has a K_2O content less than a third of that of the granophyre.

Another puzzle is why recent lavas retain excess argon and thus yield anomalously high K-Ar model ages, whereas these ancient lavas of the Cardenas Basalt and the diabase sills yield anomalously low K-Ar model ages (according to the accepted age derived in this case from a Rb-Sr isochron). If indeed these mafic rocks were 1100 Ma old, then, there has to have been significant Ar loss, yet neither the reset model for episodic Ar loss nor the leakage model for

continuous Ar loss correlates with the data, especially the ^{36}Ar data. Thus it is highly questionable whether the K-Ar system in these rocks is a valid indicator of their age.

Conclusion

Isotopic studies of the Cardenas Basalt and associated Proterozoic diabase sills and dikes have produced a geologic mystery. Using the conventional assumptions of radioisotope dating, the Rb-Sr and K-Ar systems should give concordant "ages." However, it has been known for over twenty years that the two systems give discordant "ages", the K-Ar "age" being significantly younger than the Rb-Sr "age." Previous workers have argued that a linear array of the Rb-Sr in these basalts and diabases represents a closed system. Therefore potassium, rubidium's sister alkali element, would also appear to represent a closed system. The published explanations for the discordant ages impugn the ^{40}Ar of the K-Ar system, and, at the same time, defend the Rb-Sr system. Our new data, when combined with the published data, allow models for explaining the K-Ar system to be tested.

The "argon reset model" was the first explanation proposed for the discordance. A metamorphic event is supposed to have expelled significant argon from these rocks. The reset model is unable to reconcile the new data, leading to a metamorphic event which is excessively young and inconsistent with the conventional stratigraphic interpretation of the Grand Canyon. The "argon leakage model" also attempts to explain why these rocks have about half the argon which seems to be required by the Rb-Sr system. The leakage model supposes an incredible improbability. Both the old and new data imply that the rocks leaked argon in nearly exact proportion to the abundance of potassium producing a "leakage isochron", an explanation not supported by a quantity of an appropriate mineral or mesostasis phase. Strong negative correlation between K-Ar model age and K_2O in the upper portion of the Cardenas Basalt does not find an obvious petrographic interpretation consistent with mineral phases and their degrees of alteration. Furthermore, reset and leakage models have difficulty explaining the abundance of initial ^{36}Ar in the rocks, especially the abundance of ^{36}Ar in those rocks which supposedly leaked the most ^{40}Ar.

Three alternatives are suggested to the two argon loss models. The "argon inheritance model" and "argon mixing model" simply propose that argon is positively correlated with potassium from its magma source or produced by a mixing process, and that the linear relationship on a plot of ^{40}Ar versus ^{40}K is an artifact of the magma, not produced by radioisotope decay within these rocks. Inheritance of argon is a better model for Cardenas Basalt and diabase than mixing. The "change of decay model" goes to the physics of radioisotope decay and proposes a fundamental change in ^{87}Rb and/or ^{40}K decay. All three explanations offered as alternatives to the argon loss models invalidate using the K-Ar system as conventional geochronology would assume.

References

Austin, S.A. (1994). Are Grand Canyon rocks one billion years old? In S.A. Austin (Ed.), *Grand Canyon: Monument to catastrophe* (pp.111–131). Santee, California: Institute for Creation Research.

Austin, S.A. (1996). Excess argon within mineral concentrates from the new dacite lava dome at Mount St Helens volcano. *Creation Ex Nihilo Technical Journal, 10*(3), 335–343.

Dalrymple, G.B. & Lanphere, M.A. (1969). *Potassium-argon dating: Principles, techniques and applications to geochronology*. San Francisco: W.H. Freeman.

Elston, D.P. & McKee, E.H. (1982). Age and correlation of the Late Proterozoic Grand Canyon disturbance, Northern Arizona. *Geological Society of America Bulletin, 93*, 681–699.

Ford, T.D., Breed, W.J., & Mitchell, J.S. (1972). Name and age of the Upper Precambrian Basalts in the Eastern Grand Canyon. *Geological Society of America Bulletin, 83*, 223–226.

Hammond, J.G. & Wooden, J.L. (1990). Isotopic constraints on the petrogenesis of Proterozoic diabase in Southwestern USA. In A.J. Parker, P.D. Rickwood, & D.H. Tucker (Eds.), *Mafic dykes and emplacement mechanisms* (pp.145–156). Rotterdam: Balkema.

Heaman, L.M. & Grotzinger, J.P. (1992). 1.08Ga diabase sills in the Pahrump Group, California: Implications for development of the Cordilleran Miogeocline. *Geology, 20*, 637–640.

Hendricks, J.D. (1989). Petrology and chemistry of igneous rocks of Middle Proterozoic Unkar Group, Grand Canyon Supergroup, Northern Arizona. In D.P. Elston, G.H. Billingsley, & R.A. Young (Eds.), *Geology of the Grand Canyon, Northern Arizona (with Colorado River guides)* (pp.106–116). Washington DC: American Geophysical Union.

Hendricks, J.D. & Lucchitta, I. (1974). Upper Precambrian igneous rocks of the Grand Canyon, Arizona. In T.N.V. Karlstrom, G.A. Swann, & R.L. Eastwood (Eds.), *Geology of Northern Arizona* (pp.65–86). Geological Society of America, Rocky Mountain Sectional Meeting, Flagstaff.

Hendricks, J.D. & Stevenson, G.M. (1990). Grand Canyon Supergroup: Unkar Group. In S.S. Beus & M. Morales (Eds.), *Grand Canyon geology* (pp.29–47). New York: Oxford University Press.

Howard, K.A. (1991). Intrusion of horizontal dikes: Tectonic significance of Middle Proterozoic diabase sheets widespread in the upper crust of the Southwestern United States. *Journal of Geophysical Research, 96*, 12,461–12,478.

Larson, E.E., Patterson, P.E., & Mutschler, F.E. (1994). Lithology, chemistry, age and origin of the Proterozoic Cardenas Basalt, Grand Canyon, Arizona. *Precambrian Research, 65*, 255–276.

LeBas, M.J. et al. (1986). A chemical classification of volcanic rocks based on the total alkali-silica diagram. *Journal of*

S. A. Austin & A. A. Snelling

Petrology, 27, 745–750.

Lucchitta, I. & Hendricks, J.D. (1983). Characteristics, depositional environment and tectonic interpretations of the Proterozoic Cardenas Lavas, eastern Grand Canyon, Arizona. *Geology, 11*, 177–181.

McKee, E.H. & Noble, D.C. (1974). Rb-Sr age of the Cardenas Lavas, Grand Canyon, Arizona. In T.N.V. Karlstrom, G.A. Swann, & R.L. Eastwood (Eds.), *Geology of northern Arizona* (pp. 87–96). Geological Society of America, Rocky Mountain Sectional Meeting, Flagstaff.

McKee, E.H. & Noble, D.C. (1976). Age of the Cardenas Lavas, Grand Canyon, Arizona. *Geological Society of America Bulletin, 87*, 1188–1190.

Snelling, A.A. (1998). The cause of anomalous potassium-argon "ages" for recent andesite flows at Mt. Ngauruhoe, New Zealand, and the implications for potassium-argon "dating." In R.E.Walsh (Ed.), *Proceedings of the fourth international conference on creationism* (pp. 503–525). Pittsburgh, Pennsylvania: Creation Science Fellowship.

Yoder, H.S. Jr. & Tilley, C.E. (1962). Origin of basaltic magmas: An experimental study of natural and synthetic rock systems. *Journal of Petrology, 3*, 344–532.

York, D. (1969). Least squares fitting of a straight line with correlated errors. *Earth and Planetary Science Letters, 5*, 320–324.

Appendix:
Sample Name, Location and Description

Samples whose numbers begin with "A:" are new rocks collected for K-Ar analyses by the authors. Samples whose numbers do not begin with "A:" are those with published K-Ar analyses from the geologic literature. Stratigraphic positions use the informal numbering terminology of Hendricks & Lucchitta (1974). Oxide percentages, if available, are reported on volatile free and reduced iron basis. Volcanic rock classification is according to the alkali-silica diagram after Le Bas et al. (1986).

FBM:(Bas)

Whole rock preparation of Cardenas Basalt from a random sample from the strata of Basalt Canyon collected and analyzed by Ford, Breed, & Mitchell (1972). Level within Basalt Canyon section was not specified. The rock is simply called "basalt" and is the rock on which the first published K-Ar analysis was performed.

MN:b-8

Whole rock preparation of Cardenas Basalt from Basalt Canyon collected and analyzed by McKee & Noble (1976). Near top of formation at about 270m above base; equivalent to Hendricks and Lucchitta unit 30.

MN:Tb-6

Whole rock preparation of Cardenas Basalt from Basalt Canyon collected and analyzed by McKee & Noble (1976). Near top of formation at 252m above base; equivalent to Hendricks & Lucchitta (1974) unit 28. Rock is "basaltic trachyandesite" with 55.3wt% SiO_2 and 5.4wt% total alkalis, recalculated to volatile free).

MN:b-4

Whole rock preparation of Cardenas Basalt from small canyon west of Tanner Canyon (southeast of Basalt Canyon about 2km and on the south side of the Colorado River). Collected and analyzed by McKee & Noble (1976). Equivalent to the middle of the Basalt Canyon section about 140m above base; probably equivalent to Hendricks & Lucchitta unit 11.

EM:(Pal)

Whole rock preparation of Cardenas Basalt from Palisades Creek. Analysis for K-Ar by M.L. Silberman, as reported by Elston & McKee (1982). Stratigraphic level was not specified.

LPM:4D

Whole rock preparation of Cardenas Basalt from Basalt Canyon "flow 4, upper member" collected and analyzed by Larson, Patterson, & Mutschler (1994). Probably equivalent to unit 24 of Hendricks & Lucchitta at about 220m above base. Called a "tholeiitic basalt" with 52.0wt% SiO_2 and 3.7wt% total alkalis.

LPM:4E

Whole rock preparation from a second sample of Cardenas Basalt from Basalt Canyon "flow 4, upper member" (the same flow as sample LPM:4D) collected and analyzed by Larson, Patterson, & Mutschler (1994). Probably equivalent to unit 24 of Hendricks & Lucchitta at about 220m above base. Called a "tholeiitic basalt" with 51.8wt% SiO_2 and 3.5wt% total alkalis.

A:C-1

Whole rock preparation of Cardenas Basalt from middle third of Basalt Canyon section. Equivalent to Hendricks & Lucchitta unit 9 at 103m above base. Rock is "trachyandesite" with 56.6wt% SiO_2 and 6.1wt% total alkalis. Estimated original mineral composition is plagioclase 55vol.%, augite and olivine 30vol.%, glass (mesostasis) 13vol.%, and titanomagnetite and ilmenite 2vol.%.

A:C-2

Whole rock preparation of Cardenas Basalt from middle third of Basalt Canyon section. Equivalent to Hendricks & Lucchitta unit 9 at 108m above base. A sample of the same lava flow unit as sample A:C-1. Rock is "trachyandesite" with 57.1wt% SiO_2 and 7.5wt% total alkalis. Estimated original mineral

composition is plagioclase 48 vol.%, augite and olivine 30 vol.%, glass (mesostasis)/groundmass 15 vol.%, titanomagnetite, and ilmenite 4 vol.%, orthoclase 3 vol.%, and pyrite trace.

A:C-7

Whole rock preparation of Cardenas Basalt from upper third of Basalt Canyon section. Equivalent to Hendricks and Lucchitta unit 24 at 213 m above base. Rock is "basaltic trachyandesite" with 53.9 wt% SiO_2 and 5.8 wt% total alkalis. Estimated original mineral composition is plagioclase 60 vol.%, augite 20 vol.%, olivine 5 vol.%, glass (mesostasis)/groundmass 10 vol.%, and titanomagnetite and ilmenite 5 vol.%.

A:C-10

Whole rock preparation of Cardenas Basalt from lower third of Basalt Canyon section. Equivalent to Hendricks & Lucchitta unit 7 at 83 m above base. Sample comes from center of spherical mass within more weathered and altered flow. Rock is "basaltic trachyandesite" with 53.1 wt% SiO_2 and 6.7 wt% total alkalis. Estimated original mineral composition is plagioclase 45 vol.%, augite 25 vol.%, olivine 18 vol.%, titanomagnetite and ilmenite 7 vol.%, and glass (mesostasis)/groundmass 5 vol.%.

A:C-13

Whole rock preparation of Cardenas Basalt from lower third of Basalt Canyon section. Equivalent to Hendricks & Lucchitta unit 1 at less than 1 m above the first Dox intertongue at the base of the type section. Sample is lowest flow and may be somewhat contaminated with material included from underlying Dox Formation. Rock is "tephrite basanite" with 46.6 wt% SiO_2 and 8.0 wt% total alkalis. Estimated original mineral composition is plagioclase 50 vol.%, augite 20 vol.%, olivine 15 vol.%, glass (mesostasis)/groundmass 10 vol.%, and titanomagnetite and ilmenite 5 vol.%.

A:C-14

Whole rock preparation of Cardenas Basalt from exposure on north side of Lava Chuar Canyon. Representative of the lower 50 m of the formation, the sample is probably equivalent to Hendricks & Lucchitta unit 5 about 45 m above the base of the formation. Rock is "trachyandesite" with 58.3 wt% SiO_2 and 6.8 wt% total alkalis. Estimated original mineral composition is plagioclase 45 vol.%, augite 23 vol.%, olivine 17 vol.%, glass (mesostatis)/groundmass 10 vol.%, and titanomagnetite and ilmenite 5 vol.%.

A:C-16

Whole rock preparation of Cardenas Basalt from upper third of Basalt Canyon section. Equivalent to Hendricks & Lucchitta unit 26 at 230 m above base. Sample comes from the flow just beneath the thick lapillite unit. Rock is "trachyandesite" with 57.8 wt% SiO_2 and 10.5 wt% total alkalis. Estimated original mineral composition is plagioclase 50 vol.%, augite 30 vol.%, olivine 8 vol.%, groundmass/glass (mesostasis) 7 vol.%, and titanomagnetite and ilmenite 5 vol.%.

A:C-19

Whole rock preparation of Cardenas Basalt from upper third of Basalt Canyon section. Equivalent to Hendricks & Lucchitta unit 31 at 290 m above the base. Rock is "tephrite basanite" with 47.5 wt% SiO_2 and 8.1 wt% total alkalis. Strong resemblance to sample A:C-13 which also has low silica. Estimated original mineral composition is plagioclase 45 vol.%, augite 25 vol.%, olivine 18 vol.%, groundmass/glass (mesostasis) 7 vol.%, and titanomagnetite and ilmenite 5 vol.%.

EM:(Han)

Pyroxene concentrate from the diabase sill at Hance Rapids. Collected and analyzed by Elston & McKee (1982).

EM:(Tap)

Plagioclase concentrate from the diabase sill at Tapeats Creek. Collected and analyzed by Elston & McKee (1982).

A:DI-5

Whole rock preparation from the diabase dike on the east side of Red Canyon south of Hance Rapids. Rock has 50.2 wt% SiO_2 and 5.0 wt% total alkalis. Estimated mineral composition is plagioclase 45 vol.%, olivine 30 vol.%, augite 25 vol.%, and titanomagnetite and ilmenite 5 vol.%.

A:DI-7

Whole rock preparation from the diabase sill within the Hakatai Shale at Bass Canyon on the north side of the Colorado River at mile 107.6. Rock has 47.2 wt% SiO_2 and 2.7 wt% total alkalis. Estimated mineral composition is plagioclase 45 vol.%, olivine 34 vol.%, augite 15 vol.%, titanomagnetite and ilmenite 5 vol.%, and biotite 1 vol.%.

A:DI-9

Whole rock preparation from middle of diabase sill on north side of Colorado River below Hance Rapids at mile 76.8. The sill intrudes the Bass Formation. Rock has 49.5 wt% SiO_2 and 4.6 wt% total alkalis. Estimated mineral composition is plagioclase 45 vol.%, augite 30 vol.%, olivine 20 vol.%, and titanomagnetite and ilmenite 5 vol.%.

A:DI-10

Whole rock preparation from fine-grained granophyre zone 4 m from the top of the diabase sill at Bass Canyon at mile 108 about 250 m height above the Colorado River on the north side. The sill intrudes the Hakatai Shale. Rock has 62.8 wt% SiO_2 and 9.0 wt% total alkalis. Estimated mineral composition is plagioclase 48 vol.%, quartz 25 vol.%, orthoclase 10 vol.%, augite 10 vol.%, biotite 5 vol.%, and titanomagnetite and ilmenite 2 vol.%.

A:DI-11

Whole rock preparation from same location as A:D-10 except that the rock is coarse-grained granophyre 7 m from the top of the diabase sill and about 3 to 4 m from the base of the granophyre zone. The sill intrudes the Hakatai Shale. Rock has 63.0 wt% SiO_2 and 9.5 wt% total alkalis. Estimated mineral composition is plagioclase 40 vol.%, quartz 20 vol.%, augite 15 vol.%, biotite 10 vol.%, orthoclase 8 vol.%, and titanomagnetite and ilmenite 2 vol.%.